ARTICLE

Untying a Nanoscale Knotted Polymer Structure to Linear Chains for Efficient Gene Delivery In Vitro and to the Brain

B. Newland,[a] A. Aied,[a] A. V. Pinoncely,[a] Y. Zheng,[a] T. Zhao,[a] H. Zhang,[a] R. Niemeier,[a] E. Dowd,[b] A. Pandit*,[a] W. Wang*[a]

The purpose of this study was to develop a platform transfection technology, for applications in the brain, which could transfect astrocytes without requiring cell specific functionalization and without the common cause of toxicity through high charge density. Here we show that a simple and scalable preparation technique can be used to produce a "knot" structured cationic polymer, where single growing chains can crosslink together via disulphide intramolecular crosslinks (internal cyclizations). This well-defined knot structure, can thus "untie" in reducing conditions, showing a more favorable transfection profile for astrocytes than 25kDa-PEI (48-fold), SuperFect® (39-fold) and Lipofectamine®2000 (18-fold) whilst maintaining neural cell viability at over 80% after four days of culture. The high transfection/lack of toxicity of this knot structured polymer in vitro, combined with its ability to mediate luciferase transgene expression in the adult rat brain, demonstrate its use as a platform transfection technology which should be investigated further for neurodegenerative disease therapies.

Introduction

A variety of nanoscale materials have been used to deliver nucleic acids into cells, for example nanoparticles,[1] gold nanorods[2] and functionalized carbon nanotubes.[3] These materials vary greatly in chemical composition, structure, physical properties and aspect ratio, and thus vary in delivery efficiency. Cationic polymers, also studied extensively for applications in gene delivery, show a high dependency of transfection capability on the polymer structure, even when the molecular composition is almost the same. For example, when branching is introduced into 2-(dimethylamino)ethyl methacrylate (DMAEMA) based polymers the transfection capability vastly increases compared to linear DMAEMA.[4, 5]

Living free radical polymerizations offer an attractive means to design and synthesize different structured polymers for applications in nucleic acid delivery.[6] Polymerizations such as reverse addition-fragmentation chain transfer polymerization (RAFT) or atom transfer radical polymerization (ATRP) can be used to synthesize linear homopolymers and copolymers such as block, comb and star shaped polymers. Branched/hyperbranched polymers, typically effective for nucleic acid delivery, require branching monomers or multifunctional monomers (MFM) to produce branch points. However, the Flory-Stockmayer theory statistically determines that the use of MFMs will inevitably lead to crosslinking and gelation.[7, 8] These MFMs can therefore only be incorporated in very small amounts (typically less than 1%)[9] resulting in few branch points among long linear chains.[10] In contrast, our recently proposed kinetic theory, introduced to supplement the Flory-Stockmayer theory, suggests that actually MFMs can be used in large proportions (even homopolymerisation) if the boundary of a growing chain in any active cycle is kept very small.[11] Thus, in a reaction such as deactivation enhanced ATRP (DE-ATRP), a reduced instantaneous growth boundary can be obtained whereby growing chains of MFM no longer crosslink to different chains (intermolecular crosslinks) until much later in the reaction process.[11] Instead single chains grow and link to themselves (intramolecular cyclisations) to form a single cyclized knot polymer structure.

We have previously demonstrated the gene delivery potential of non-degradable single cyclized knot structures over a range of cell types.[12] The 3-dimentional polymer structure does result in a high transfection capability but the associated toxicity increased when the molecular weight of the knots reached a level suitable for optimal transfection (25-30kDa). A vast improvement over the previous knot polymer was sought, that would not show cellular toxicity at the required polymer/plasmid ratio, but would remain highly efficient, thus breaking the trend of the vehicle efficiency/toxicity relationship. It was hypothesized that a high molecular weight knot structure, with cleavable crosslinks, would allow for the high transfection capability associated with the dense 3D structure, but maintain cellular viability via polyethylene glycol (PEG) units and intracellular cleavage (untying to linear chains). Lastly, it was desired to analyse whether this

transfection agent could provide a platform technology for use in the context of brain/central nervous system (CNS) applications through its simplicity, scalability and option of post synthesis modifications.

Experimental

Materials

The monomers 2-(dimethylamino)ethyl methacrylate (DMAEMA) and poly(ethylene glycol) methyl ethyl methacrylate (PEGMEMA) were purchased from Sigma Aldrich. The third monomer, composed of a disulphide linked dimethacrylate (DSDMA), was synthesized as previously reported by Li and Armes.[13] The reagents bis(2-hydroxyethyl) disulfide (BHEDS), triethylamine and methacryloyl chloride for DSDMA synthesis were purchased from Sigma Aldrich. N-pentamethyldiethylenetriamine (PMDETA, 99%), ethyl 2-bromoisobutyrate (EBriB, 98%), copper(II) chloride ($CuCl_2$, 97%), d-Chloroform (99.8%), L-ascorbic acid (AA, 99%) and hydrochloric acid (HCl, 37%) were used as received from Sigma Aldrich. 2-Butanone (HPLC grade, LabScan), tetrahydrofuran (THF, HPLC grade, Fisher), n-hexane (ACS reagent grade, Fisher), dichloromethane (ACS reagent grade, Fisher) and dimethylflormamide (DMF, HPLC grade, Fisher) were used as received. For analysis of the polyplexes, agarose (for electrophoresis, Aldrich), SYBR® Safe Gel stain (Invitrogen), BioLux™ Gaussia Luciferase Assay Kit (New England Biolabs), alamarBlue® (Invitrogen) were used as received and according to manufacturers' protocols.

Synthesis of DSP8

In situ deactivation enhanced atom transfer radical polymerization (DE-ATRP) was used to allow sufficient control for intramolecular cyclization to occur. The initiator EBriB (9.2 mg, 1 molar equivalent), the catalyst $CuCl_2$ (3.8 mg, 0.6 molar equivalent) and the catalyst ligand PMDETA (4.9 mg, 0.6 molar equivalent) were added into a 2-necked round bottom flask. Monomers were added in the following ratio: DMAEMA 5.95 g, 820 molar equivalents, PEGMEMA 1.75 g, 80 molar equivalents and DSDMA 0.91 g, 100 molar equivalents. After removal of oxygen, 20 µl of 36mg/ml AA(aq), 0.09 molar equivalent was added under positive pressure of argon to begin the polymerization at 40ºC with stirring set at 800rpm (flask suspended in a pre-heated oil bath). The reaction was stopped by opening the flask to the air and swirling the contents to allow oxygen through the liquid.

Purification of DSP8

All stages of the following purification process were performed in the absence of direct light where possible. The polymer was diluted in THF, then precipitated using an excess of vigorously stirring hexane. The hexane was then removed and the polymer was left to dry under laminar flow. This was then re-dissolved in acetone and the pH was reduced to 5 by adding 1M HCl before immediate dialysis against dH_2O using a Spectrapor® dialysis membrane (6000-8000 MWCO) for several days. Finally the polymer was freeze dried to a white powder for subsequent analysis.

Determination of Molecular Weight

During the reaction process, 1 ml samples were extracted under positive argon pressure for gel permeation chromatography (GPC) analysis of the molecular weight. The samples were diluted in DMF then filtered through aluminia for chromatography then through a 0.2 µm pore filter. The molecular weight and polydispersity index of each sample was determined using a Varian 920-LC instrument with a refractive index detector. DMF was used as the eluent and chromatograms were run at 50°C using with a flow rate of 1 ml/min. The machine was calibrated with linear polystyrene standards.The main text of the article should go here with headings as appropriate.

1H-Nuclear Magnetic Resonance (NMR) Spectroscopy Analysis

A sample of the polymer was dissolved in 2 ml of D_2O for ^{1}H-NMR analysis at 300 MHz using a Bruker spectrometer. All chemical shifts are reported in ppm relative to TMS.

Polyplex Characterisation

Gaussia princeps luciferase plasmid DNA (pCMV-G Luc) was purchased from New England BioLabs, and was expanded and purified using the Giga-Prep (Qiagen) kit as per protocol. The polyplex formed with pCMV-G Luc and DSP8 were characterized by gel electrophoresis and size/charge analysis. Polyplexes were formed using 10 µg of plasmid DNA, and varying weight ratios of polymer, made to a final volume of 100 µl in H_2O for size analysis with a zetasizer (Malvern Instruments). Each sample was then diluted with H_2O to a total of 700 µl for charge analysis. Three repeat experiments were made for size charge analysis and an average value plotted. 5 µl of this polyplex solution was added to 5 µl of loading buffer and added to wells of a 0.8% agarose gel in Tris-borate-EDTA (TBE) buffer with SYBR®Safe DNA stain and subjected to 80 mV for 20 minutes. The movement of the DNA through the gels was visualized using a G:Box (Syngene) and associated GeneSnap software.

Cytotoxicity Analysis

The LC50 values were calculated for the polymers PEI and DSP8 by adding varying concentrations of polymer solutions (made up in the normal growth media) to Neu 7 astrocytes for 24 hours and analysing the cell viability at each concentration using the alamarBlue® reduction technique described in the following section. The concentration that caused a 50% decrease in cell viability (LC50) was read from the cell viability vs polymer concentration plot and recorded.

In addition the LIVE/DEAD® Cell Viability (Molecular Probes®) assay was carried out according to the manufacturer's protocol, on Neu 7 cells seeded on poly-L-lysine coated glass coverslips, 24 hours after polyplex or naked DNA treatment. The assay measures intracellular esterase activity via green-fluorescent calcein-AM and membrane integrity via red-fluorescent ethidium homodimer-1.

Transfection and Cytotoxicity Analysis

The Neu 7 astrocyte cell line was cultured in low glucose Dulbecco's Modified Eagles Medium (DMEM)(Sigma Aldrich) supplemented with filtered fetal bovine serum 10% (FBS) (Sigma Aldrich) and 1% Penicillin/Streptomycin (P/S) (Sigma Aldrich) at 37ºC, 5% CO_2 humidified atmosphere and using standard sterile techniques. 24 hours prior to experimentation,

the cells were trypsinized, and seeded at a density of 10,000 cells/well in a 96-well plate. 10 µl of polyplexes, containing 1 µg of DNA, were made up in dH_2O as described above and added to the 100 µl of the media in each well of the 96-well plate. All experiments were therefore carried out in the presence of serum. After 24 hours of incubation with the polyplexes the media was removed for analysis using the G-Luciferase enzymatic assay (New England BioLabs) according to the manufacturer's protocol. The luminescence was immediately read using a Varioskan plate reader (Thermo Scientific). In the meantime, to analyse the cell viability, the cells in the test well were washed with Hanks Balanced Salt Solution (HBSS)(Sigma Aldrich) and 100 µl of a 10% alamarBlue® solution in HBSS was added to each well and incubated for a further three hours. The absorbance of the reduced solution was then read at 595 and 550nm and converted to a percentage of cell viability by normalizing to the Naked DNA treatment group. For the time course study, the 100 µl of cell supernatant was removed at day 1,2 and 4 for analysis, each time being replaced with 10% alamarBlue® solution in HBSS for the cytotoxicity analysis, followed by a wash and fresh media applied until the next time point.

Transfection Analysis in the Rat Brain

All procedures were approved by the Animal Ethics Committee of the National University of Ireland, Galway and were carried out in accordance with the European Communities Council Directive (86/609/EEC). A total of 12 adult male Sprague Dawley rats (Charles Rivers, UK) weighing between 250-275g on the day of surgery were used and randomly assigned to groups for intraventricular injections. Rats were deeply anesthetised using gaseous isoflurane (2-5% in oxygen), and mounted via ear and teeth bars. Bilateral injections into the lateral ventricles were made via the following stereotactic coordinates: Anteroposterior -0.9 mm, Mediolateral ±1.6 mm (from Bregma) and Dorsoventral -3.5 mm (from Dura). 2µl of naked DNA or polyplexes containing 1 µg of DNA prepared in dH_2O was delivered to each injection site. Delivery was controlled at a rate of 1µg/min by a syringe pump, and the cannula remained in place for an additional two minutes to allow diffusion from the cannula tip before removal.

Tissue Processing

48 hours post injection, rats were deeply anesthetized by intraperitoneal injection of pentobarbital (100 mg per kg bodyweight) followed by decapitation. Brains were immediately removed and frozen immediately over dry ice. The brains were later thawed, the cerebellum and olfactory bulbs were removed, the hemispheres were then divided and homogenised individually in 1 ml of Cell-Lytic™ lysis buffer (Sigma Aldrich). 100 µl of each sample was then analyzed using the luciferase assay kit as per manufacturer's protocol.

Statistical Analysis

GraphPad Prism 5 software was used to perform all statistical analyses. A one way ANOVA was performed using Tukey's post hoc test to compare all groups. P values < 0.05 were considered significantly different. For the *in vivo* analysis an ANOVA was performed with a Dunn's multiple group analysis, P values < 0.05 were considered significantly different.

Results and Discussion

Scheme 1 shows a depiction of the DE-ATRP reaction process used to form the knot polymer. The disulphide dimethacrylate monomer (DSDMA) shown in Scheme 1 and SI Figure 1 (Supporting Information) was synthesized as previously described by Li and Armes.[13] DSDMA, DMAEMA and polyethylene glycol methyl ether methacrylate (PEGMEMA) were combined in the following ratio 10:82:8 respectively. The monomer to initiator (ethyl 2-bromoisobutyrate) ratio was 1000:1 to produce a predominantly single chains knotted to themselves (cyclized knot structure). During the reaction process, single chains grow, and due to both the presence of di-vinyl monomers and the reduced growth boundary effect mediated by DE-ATRP, these chains only crosslink to themselves. This forms a single chain knotted to itself in via intramolecular crosslinks every 18 monomers of the chain (5.6% branching – see Supplementary Table S1). This synthesis strategy results in a polymer with low polydispersity even at high molecular weights (PDI = 1.44, M_w= 30 kDa) (see Supplementary Information Table S2), with molecular weight increasing almost linearly with monomer conversion (Figure 1 insert). The gel permeation chromatography (GPC) peaks remain narrow and highly symmetrical throughout the growth process. Careful examination of each peak shows that the tails of each (right hand side (lowest M_w)) shift to the left as would a growing linear chain. During chain combination (hyperbranched polymers), this typically remains more static and the peaks broaden as the polymers become ever-more polydisperse[10]. However, in our system, the PDI remains low, and the peaks move uniformly to the right as would a linear grown. This linear-like chain growth, although seemingly like that of the growth of a linear polymer, does in fact result in approximately one third of the di-vinyl monomers being used as branching agents (therefore within the same chain) (Supplementary Table S1) thus the formation of the single cyclized knot; henceforward termed DSP8 (with 8 representing the percentage PEG feed ratio).

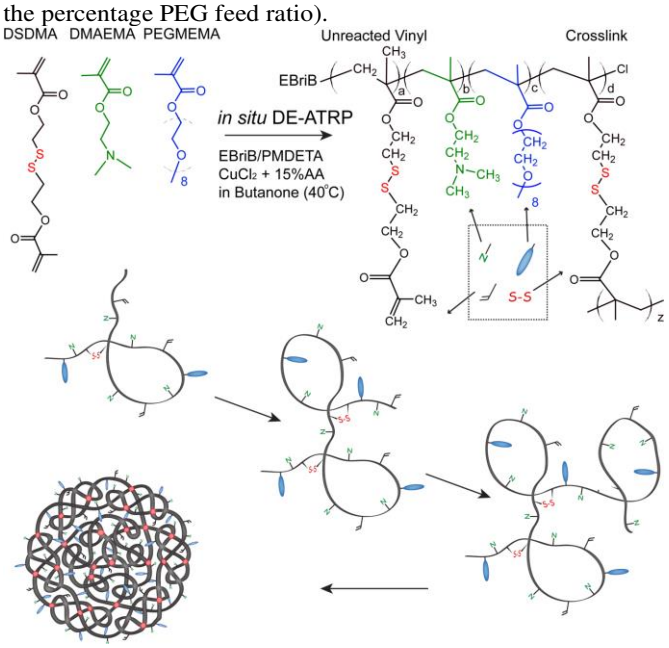

Scheme 1 Formation of the cyclized knot polymer via DE-ATRP. The monomers disulphide dimethacrylate (DSDMA), 2-(dimethylamino) ethyl methacrylate (DMAEMA) and poly(ethylene glycol) methyl ether methacrylate (PEGMEMA) form a single growing chain that crosslinks to itself (intramolecular crosslinks) via DSDMA. The scheme depicts this single growing chain and how it can link to itself, although the final structure is of course not symmetrical or ordered as shown graphically.

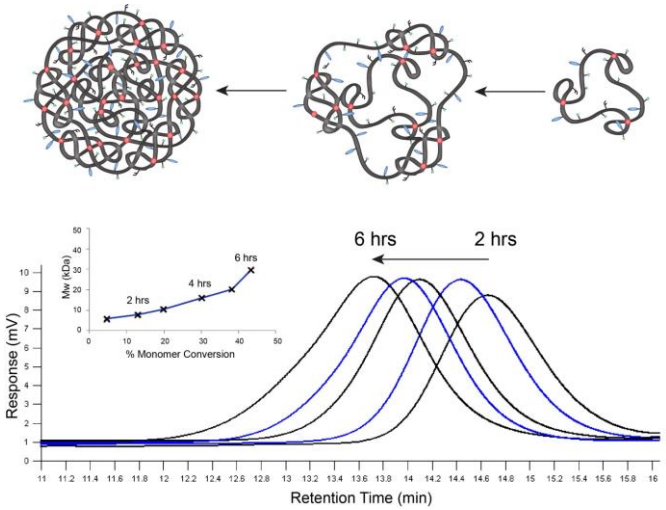

Figure 1 Controlled growth of the knot structure. Gel permeation chromatography peaks and corresponding schematic diagrams (though no order or symmetry assumed in the knot structure) of samples taken during the reaction stages show the formation of the single cyclized knot through intramolecular crosslinks (depicted in red) after six hours (M_w = 30.0 kDa, PDI = 1.44). Note the shift of the peak tails towards the left and the graphical insert of M_w change vs percentage conversion, both showing the linear like growth of single chains.

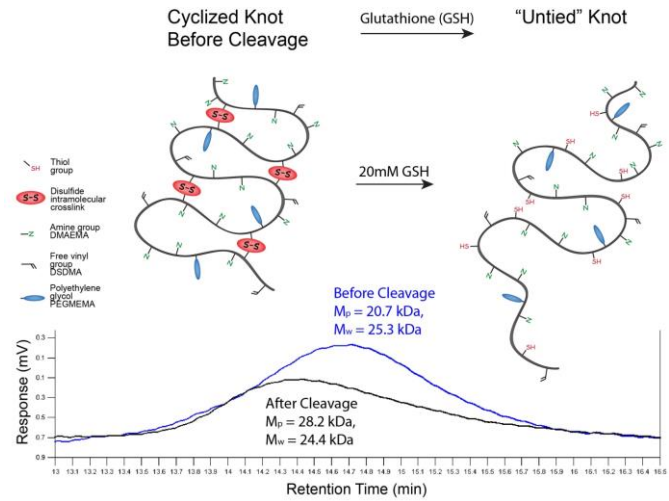

Figure 2 Untying the knot. Gel permeation chromatography peaks and schematic diagrams shows the change in molecular weight after treating the polymer samples with 20 µM glutathione (GSH). Cleaving the intramolecular crosslinks (depicted in red) effectively unties the knot structure resulting in little change in the molecular weight, but a shift of the peak molecular weight (Mp) to the left as the untied knot has a larger hydrodynamic volume.

^{1}H NMR spectroscopy analysis of DSP8 reveals free vinyl groups (11.6%) are also present in the knot structure (Supplementary Table S1). This vinyl functionality could potentially be used for attaching targeting moieties or adding end capping agents through Michael type addition. Degradation of the purified polymer in 20 µM glutathione or 20 µM tris(2-carboxyethyl) phosphine (TCEP) did not result in a large decrease in molecular weight (from 25.3 kDa to 24.4 kDa, (Figure 2) as the intramolecular knot crosslinks were cleaved. In fact there was an increase in the peak molecular weight (Mp) from 20.7 kDa to 28.2 kDa showing the increase in hydrodynamic volume (less density) occupied by the untied

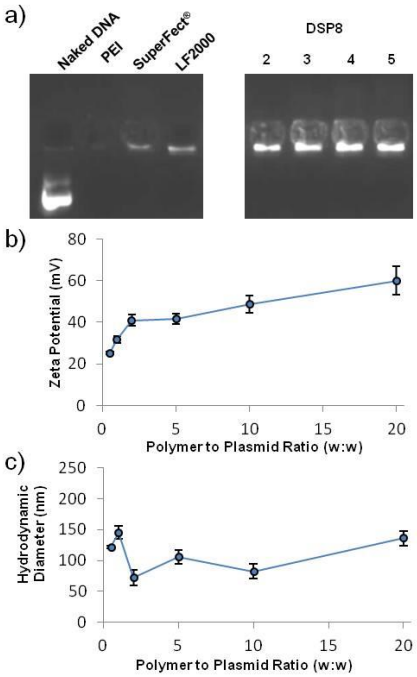

Figure 3 Polyplex characterisation: **a)** shows retardation of DNA through the agarose gel at all polymer/plasmid weight ratios analyzed along with PEI (2:1 w:w) polyplexes, SuperFect® (8:1 w:w) polyplexes and Lipofectamine 2000 (3:1 w:w) lipoplexes. Surface charge increased upon increasing polymer to plasmid ratio **b)**, and polyplex sizes, via dynamic light scattering, vary with little apparent trend **c)**.

linear chains. It should be noted here that this polymer structure is distinctly different from either linear,[14] hyperbranched[15] or dendrimer cations[16] traditionally used for non-viral gene transfection. It is the product of a highly controlled reaction involving only the addition of monomers to the growing chain, or internal cyclization reactions.

The electrostatic interaction between cationic polymers and negatively charged nucleic acids condenses the genetic material into nanoscale particles (polyplexes). Polyplexes formed with knot polymers typically show high resistance to DNase degradation[12, 17] and were characterised here in terms electrophoretic mobility, size and charge. Figure 3a shows that polyplexes could successfully be formed at a 2:1 polymer to plasmid weight ratio, or higher, as shown by the hindrance of mobility through the agarose gel. Size/charge analysis (Figure 3b and c) showed polyplexes increased in charge with increasing polymer/plasmid ratio (between 25 and 60 mV) but showed a variety of sizes between (70-150 nm).

The ability to transfect "hard to transfect" tissue such as the brain or CNS could have profound implications for the future treatment of neurodegenerative disorders such as Alzheimer's disease and Parkinson's disease. Astrocytes are a predominant cell type of the brain, present in proximity to dopaminergic neurons (those lost in Parkinson's disease). Studies have therefore focused on the delivery of secreted growth factors such as glial cell line-derived neurotrophic factor (GDNF) encoding DNA to surrounding astrocytes, rather than to neurons themselves.[17] However, transfection of astrocytes can be difficult, necessitating specific tailoring of the polymer composition.[18] Transfection of the neuronal cell types by non-viral means remains a difficult challenge, one which has seen a shift of focus towards silencing RNA technology[3, 19, 20] because of the relative ease of silencing the translation of mRNA into

protein. However, overexpression of therapeutic genes/proteins in the degenerating brain holds significant promise and should not be overlooked.[21, 22]

The Neu 7 astrocyte cell line used to analyse the cytotoxicity and transfection capability of DSP8 was developed as an astrocyte that produces a neuroinhibitory environment,[23] somewhat typical to that of damaged CNS tissue. Previous studies have shown Neu 7 astrocytes to be amenable to transfection[17] so they were chosen for the following studies to analyze the performance of the knot polymer in comparison to commercially available polymers. Whilst improving the transfection efficiency of non-viral vectors remains a necessity, analysis of the material toxicity is of equal importance. Nanoscale materials may have safety issues due to a high aspect ratio[24] or an inherent charge density, causing toxicity to the brain.[25] Thus, the toxicity of DSP8 was specifically studied via combination of methods in polyplex form or free solution.

The concentration at which DSP8 causes a 50% reduction in cell viability (LC50) was measured in comparison to 25kDa branched polyethyleneimine. Polymer solutions, without being complexed to DNA, were analysed using the alamarBlue® assay 24 hours after the addition of concentrations ranging from 1 µg/ml to 500 µg/ml. Figure 4a shows a large difference between the toxicity profile of DSP8 (LC50 = 339 µg/ml) compared to PEI (LC50 = 11 µg/ml). This elevated toxicity of PEI could also be observed for PEI polyplexes formed with 1 µg of DNA, as observed in the fluorescent micrographs of the LIVE/DEAD® assay (Molecular Probes®) (Figure 4b), whereby dead cells, stained with red-fluorescent ethidium homodimer-1 were present and there were large areas cleared of green-fluorescent calcein-AM stained healthy cells. SuperFect® polyplexes (Figure 4c) allowed a greater portion of live cells then PEI polyplexes, but had more dying cells than DSP8 polyplexes (Figure 4d). Both PEI and SuperFect® have no cleavable units nor the ability to biodegrade. However, due to the presence of disulfide bonds within the polymer structure, it is likely that DSP8 changes conformation upon cell entry. Less dense linear chains should form, exhibiting low toxicity. This vast difference in cytotoxicity could have large implications for the clinical translation of such non-viral vectors, where lack of toxicity will be of paramount importance.

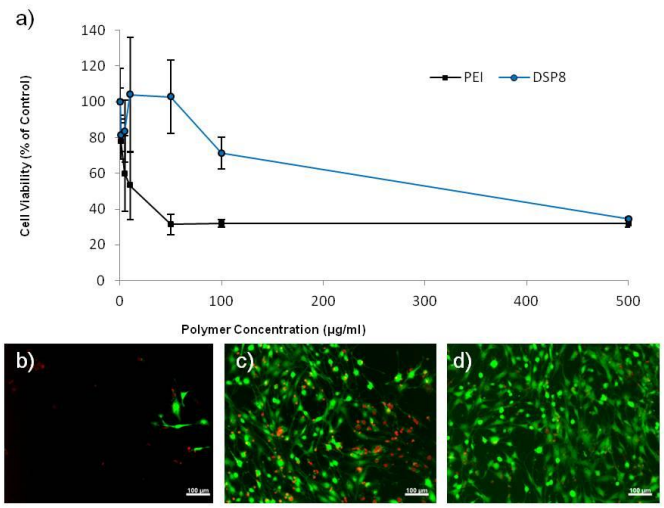

Figure 4 Cytotoxicity of DSP8 towards Neu7 astrocytes in comparison to control transfection agents. **a)** Determination of the LC50 value for DSP8 in comparison to PEI using increasing concentrations of the polymer solution and the alamarBlue® assay. Representative images of LIVE/DEAD® analysis following treatment with polyplexes formed with **b)** PEI, **c)** SuperFect® or **d)** DSP8, 24hours post treatment, n=4.

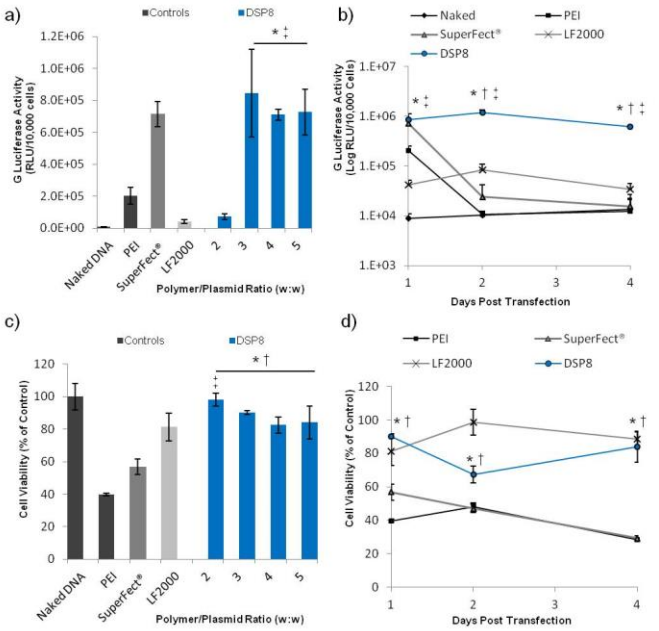

Figure 5 Transfection and cell viability analysis with Neu 7 astrocytes. Luciferase transgene levels 24 hours post transfection **a)** or up to four days post transfection **b)** with the knot polymer DSP8 in comparison to commercially available controls. Cell viability analysis 24 hours **c)** or up to four days **d)** post transfection (3:1 ratio for DSP8) as analyzed using the alamarBlue® assay. Four days post transfection, DSP8 exhibited 48, 39 and 17 fold higher transgene expression than PEI, SuperFect® and Lipofectamine® 2000 respectively, and two fold increase in cell viability over PEI and SuperFect. All studies carried out in the presence of serum, n=4, symbols mark statistically significant difference ($P<0.05$) from PEI (*), SuperFect® (†), and Lipofectamine® 2000 (‡) (one way ANOVA, Tukey's post hoc analysis).

The transfection capability and cytotoxicity of the polyplexes formed with DSP8 were then analysed over a period of four days. The duration of transgene expression was investigated, because, for applications for neurological disorders, extended transgene expression time would be favourable.[26] Figure 5a shows that as early as 24 hours post administration, all bar one of the weight ratios for DSP8 gave significantly higher luciferase transfection levels than the "gold standard" branched 25kDa PEI. Furthermore, Figure 5b shows that at two days and four days post transfection the luciferase expression levels produced by DSP8 polyplexes are far higher than those of PEI, the SuperFect® PAMAM dendrimer and the commonly used lipid based Lipofectamine® 2000. Two days post transfection DSP8 luciferase levels are 111 times, 50 times, and 14 times higher than PEI, SuperFect® and Lipofectamine® 2000 respectively. By four days post transfection the DSP8 luciferase levels had decreased slightly, but were still 48 times, 39 times and 18 times that of PEI, SuperFect® and Lipofectamine® 2000 respectively.

Whilst much research results in incremental gains in the performance of non-viral gene vectors, this knot structure shows a profound increase in the luciferase expression compared to current commercially available transfection agents. The luciferase expression levels produced by the knot polymer and Lipofectamine® 2000 stay approximately level over the analysis period, but the expression due to the PEI and SuperFect® controls decreases, presumably through the toxicity mediated by these polymers. Figure 5c shows that over 80% cell viability is maintained after the addition of DSP8 polyplexes (containing 1 µg of DNA per well) at the

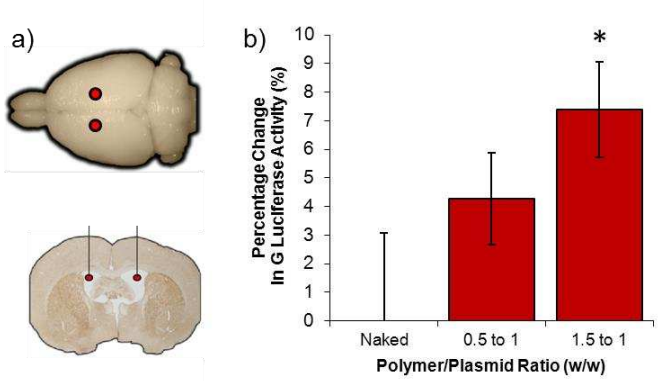

Figure 6 Luciferase transgene activity in the rat brain. Direct intraventricular delivery (depicted in **a**)) of DSP8 polyplexes at a ratio of 1.5:1 resulted in a 7.4% increase in luciferase activity over the naked DNA control **b)**. n=3, * marks statistically significant difference ($p<0.05$) from naked DNA group (Kruskall-Wallis test with Dunn's multiple group analysis, $p=0.0390$, Kruskall-Wallis statistic = 6.489).

polymer/plasmid ratios tested which are all statistically significantly different to that of PEI (40% viability) and SuperFect® (57% viability). This improved cell viability is also observed at the two and four day time points post transfection (Figure 5d).

Research into the development of non-viral vectors for applications in neurodegenerative diseases has more recently focused on the addition of a variety of moieties to improve the transfection process.[27] Molecules such as transferrin have been used to aid delivery across the blood brain barrier[28] or to increase the transfection capability of liposomes stereotactically injected into the rodent brain.[19] Neuron targeting moieties such as Tet1 have also been added to polymeric vectors allowing greater neuronal cell transfection than unmodified polymers.[29] However, despite these continual incremental improvements shown by the post synthesis addition of moieties, we aimed to synthesize and analyse a platform transfection technology that would be highly effective in an unmodified form.

The ability to design a platform transfection technology, which could be simple to synthesize, but allow individual tailoring to specific target tissues was desired. Thus the ability of DSP8 to mediate luciferase expression in the brain was analysed via direct stereotactic injection into the lateral ventricle (connecting large areas within the brain). Figure 6 shows that the administration of DSP8 polyplexes directly into the ventricle of the adult Sprague Dawley rat mediates a 7.4% increase in the level of transgene expression over naked DNA two days post injection. A previous study by Pun and co-workers has shown that non-viral transfection can be achieved in the rodent brain via intraventricular injection, which occurred predominantly in the subventricular zone.[29] Figure 6b shows that an increased level of transfection can be achieved using DSP8 at a polymer plasmid ratio of 1.5 to 1 (w:w). The increase in transgene expression observed, proves the concept that non-targeted polymers can be used to deliver DNA to the brain, but that it is likely to benefit from the addition of specific targeting moieties. Clearly DSP8 requires vast improvements, and is far from the CNS transfection efficiencies of adeno-associated viruses such as those used in intracerebral clinical trials. DSP8 will therefore indeed require further modification if it is to deliver therapeutic genes with efficiencies capable of functional improvements in animal models of neurodegenerative diseases. However, the presence of vinyl functionality within the knot structure (Supplementary Figure S2) still allows the possibility of further modification (e.g. via standard click chemistry) with endcapping moieties,[30] targeting peptides,[29] or antibody fragments.[31] Ongoing studies in our lab aim to create functionalised knot polymers specifically for enhanced neuronal transfection.

Conclusions

The simplicity of DE-ATRP for large scale synthesis of this knot structured polymer, the high transfection capability and the lack of toxicity demonstrates its use as a platform transfection technology. Analysis of the polymer degradation profile indirectly demonstrates the cleavable cyclized knot structure as the knot becomes "untied" when the intramolecular crosslinks are cleaved. DSP8 showed far lower levels of cytotoxicity than PEI with a ~20 fold difference in LC50 values. Cytotoxicity analysis showed that the astrocyte viability remained above 80% when treated with DSP8 polyplexes at the weight ratios tested, compared with a decrease shown by both PEI and SuperFect® polyplexes. The transgene expression mediated by DSP8 supersedes that of PEI and Lipofectamine® 2000, and continues up to four days post transfection at a level 48 fold higher than PEI, 39 fold higher than the SuperFect® PAMAM dendrimer and 18 fold higher than the commonly used Lipofectamine® 2000. In summary, the good transfection profile and low cytotoxicity shown in astrocytes shows the potential of such a knot structure for gene delivery. Furthermore, the ease of this "one-pot" synthesis allows a variety of parameters such molecular weight, degree of PEGylation and moiety addition to be easily tailored for specific applications.

Acknowledgements

The authors wish to thank Science Foundation of Ireland (SFI), Strategic Research Cluster (SRC) (grant no. 07/SRC/B1163), SFI Principal Investigator programme, Heath Research Board (HRB) of Ireland, DEBRA Ireland and National University of Ireland, Galway for financial support.

Notes and references

[a] Network of Excellence for Functional Biomaterials (NFB), National University of Ireland, Galway, Ireland.

[b] Pharmacology and Therapeutics, National University of Ireland, Galway, Ireland.

† Electronic Supplementary Information (ESI) available: [^{1}H NMR Spectroscopy Data and Gel Permeation Chromatography Data]. See DOI: 10.1039/b000000x/

1. H. Lee, A. K. R. Lytton-Jean, Y. Chen, K. T. Love, A. I. Park, E. D. Karagiannis, A. Sehgal, W. Querbes, C. S. Zurenko, M. Jayaraman, C. G. Peng, K. Charisse, A. Borodovsky, M. Manoharan, J. S. Donahoe, J. Truelove, M. Nahrendorf, R. Langer and D. G. Anderson, *Nature Nanotech.*, 2012, **7**, 389-393.
2. A. C. Bonoiu, E. J. Bergey, H. Ding, R. Hu, R. Kumar, K.-T. Yong, P. N. Prasad, S. Mahajan, K. E. Picchione, A. Bhattacharjee and T. A. Ignatowski, *Nanomedicine,* 2011, **6**, 617-630.
3. K. T. Al-Jamal, L. Gherardini, G. Bardi, A. Nunes, C. Guo, C. Bussy, M. A. Herrero, A. Bianco, M. Prato, K. Kostarelos and T. Pizzorusso, *Proc. Natl. Acad. Sci. USA*, 2011, **108**, 10952-10957.

4. A. Schallon, V. Jérôme, A. Walther, C. V. Synatschke, A. H. E. Müller and R. Freitag, *Reac. Func. Polym.*, 2010, **70**, 1-10.
5. B. Newland, H. Tai, Y. Zheng, D. Velasco, A. Di Luca, S. M. Howdle, C. Alexander, W. Wang and A. Pandit, *Chem. Commun.*, 2010, **46**, 4698-4700.
6. D. S. H. Chu, J. G. Schellinger, J. Shi, A. J. Convertine, P. S. Stayton and S. H. Pun, *Acc. Chem. Res.*, 2012, **45**, 1089-1099.
7. P. J. Flory, *J. Am. Chem. Soc.*, 1941, **63**, 3083-3090.
8. W. H. Stockmayer and H. Jacobson, *J. Chem. Phys.*, 1943, **11**, 393-393.
9. L. Wang, C. Li, A. J. Ryan and S. P. Armes, *Adv. Mater.*, 2006, **18**, 1566-1570.
10. T. Zhao, Y. Zheng, J. Poly and W. Wang, *Nature Commun.*, 2013, **4**, 1873.
11. Y. Zheng, H. Cao, B. Newland, Y. Dong, A. Pandit and W. Wang, *J. Am. Chem. Soc.*, 2011, **133**, 13130-13137.
12. B. Newland, Y. Zheng, Y. Jin, M. Abu-Rub, H. Cao, W. Wang and A. Pandit, *J. Am. Chem. Soc.*, 2012, **134**, 4782-4789.
13. Y. Li and S. P. Armes, *Macromolecules*, 2005, **38**, 8155-8162.
14. M. Breunig, U. Lungwitz, R. Liebl and A. Goepferich, *Proc. Natl. Acad. Sci. USA*, 2007, **104**, 14454-14459.
15. R. Reul, J. Nguyen and T. Kissel, *Biomaterials*, 2009, 30, 5815-5824.
16. J. L. Santos, H. Oliveira, D. Pandita, J. Rodrigues, A. P. Pêgo, P. L. Granja and H. Tomás, *J. Control. Release*, 2010, **144**, 55-64.
17. B. Newland, M. Abu-Rub, M. Naughton, Y. Zheng, A. V. Pinoncely, E. Collin, W. Wang and A. Pandit, *ACS Chem. Neurosci.*, 2013, **4**, 540-546.
18. S. Y. Tzeng, H. Guerrero-Cázares, E. E. Martinez, J. C. Sunshine, A. Quiñones-Hinojosa and J. J. Green, *Biomaterials*, 2011, **32**, 5402-5410.
19. A. L. C. Cardoso, P. Costa, L. P. de Almeida, S. Simões, N. Plesnila, C. Culmsee, E. Wagner and M. C. Pedroso de Lima, *J. Control. Release*, 2010, **142**, 392.
20. L. Alvarez-Erviti, Y. Seow, H. Yin, C. Betts, S. Lakhal and M. J. A. Wood, *Nature Biotech.*, 2011, **29**, 341-345.
21. W. J. Marks Jr, R. T. Bartus, J. Siffert, C. S. Davis, A. Lozano, N. Boulis, J. Vitek, M. Stacy, D. Turner and L. Verhagen, *Lancet Neurol.*, 2010, **9**, 1164-1172.
22. P. A. LeWitt, A. R. Rezai, M. A. Leehey, S. G. Ojemann, A. W. Flaherty, E. N. Eskandar, S. K. Kostyk, K. Thomas, A. Sarkar, M. S. Siddiqui, S. B. Tatter, J. M. Schwalb, K. L. Poston, J. M. Henderson, R. M. Kurlan, I. H. Richard, L. Van Meter, C. V. Sapan, M. J. During, M. G. Kaplitt and A. Feigin, *Lancet Neurol.*, 2011, **10**, 309-319.
23. L. C. Smith-Thomas, J. Fok-Seang, J. Stevens, J. S. Du, E. Muir, A. Faissner, H. M. Geller, J. H. Rogers and J. W. Fawcett, *J. Cell Sci.*, 1994, **107**, 1687-1695.
24. C. A. Poland, R. Duffin, I. Kinloch, A. Maynard, W. A. H. Wallace, A. Seaton, V. Stone, S. Brown, W. MacNee and K. Donaldson, *Nature Nanotech.*, 2008, **3**, 423-428.
25. B. Newland, T. C. Moloney, G. Fontana, S. Browne, M. T. Abu-Rub, E. Dowd and A. S. Pandit, *Biomaterials*, 2013, **34**, 2130-2141.
26. D. M. Yurek, A. M. Fletcher, G. M. Smith, K. B. Seroogy, A. G. Ziady, J. Molter, T. H. Kowalczyk, L. Padegimas and M. J. Cooper, *Mol. Ther.*, 2009, **17**, 641-650.
27. B. Newland, E. Dowd and A. Pandit, *Biomaterials Science*, 2013, **1**, 556-576.
28. N. Shi, Y. Zhang, C. Zhu, R. J. Boado and W. M. Pardridge, *Proc. Natl. Acad. Sci. USA*, 2001, **98**, 12754-12759.
29. E. J. Kwon, J. Lasiene, B. E. Jacobson, I.-K. Park, P. J. Horner and S. H. Pun, *Biomaterials*, 2010, 31, 2417-2424.
30. J. J. Green, G. T. Zugates, N. C. Tedford, Y. H. Huang, L. G. Griffith, D. A. Lauffenburger, J. A. Sawicki, R. Langer and D. G. Anderson, *Adv. Mater.*, 2007, **19**, 2836-2842.
31. M. Monaghan, U. Greiser, H. Cao, W. Wang and A. Pandit, *Drug Deliv. Trans. Res.*, 2012, **2**, 406-414.